Absorption of Flue-Gas Components by Ionic Liquids

Kolding, Helene; Thomassen, Peter Langelund; Mossin, Susanne; Kegnæs, Søren; Riisager, Anders; Rogez, Jaques; Mikaelian, G.

Published in:
E C S Transactions

Link to article, DOI:
10.1149/06404.0097ecst

Publication date:
2014

Document Version
Peer reviewed version

Absorption of Flue-Gas Components by Ionic Liquids

H. Kolding[a], P. Thomassen[a], S. Mossin[a], S. Kegnæs[a], A. Riisager[a], J. Rogez[b], G. Mikaelian[b], and R. Fehrmann[a]

[a]Centre for Catalysis and Sustainable Chemistry, Department of Chemistry, Technical University of Denmark, DK-2800 Kgs. Lyngby, Denmark
[b]TECSEN, UMR6122, CNRS-Université Paul Cezanne, Aix-Marseille III, France

Gas separation by ionic liquids (ILs) is a promising new research field with several potential applications of industrial interest. Thus cleaning of industrial off gases seems to be attractive by use of ILs and Supported Ionic Liquid Phase (SILP) materials. The potential of selected ILs for absorption of NO_X, CO_2 and SO_2 are demonstrated and the possible mechanism of absorption described on the molecular level. Special focus regards the interaction of the ILs with water vapor, which is an important feature in envisaged application of flue gas cleaning in power plants, waste incineration plants, cement and glass factories as well as on board ships.

Introduction

A major concern in relation to atmospheric pollution and climate changes is emission of acidic gases such as NO_X, SO_X and CO_X from combustion of fossil fuels in, e.g. power plants. Accordingly, these gases have to be effectively removed from flue gases. Presently this is mainly achieved by relatively energy intensive and resource demanding technologies via selective catalytic reduction (SCR) of NO_X with ammonia, SO_2 wet-scrubbing by lime obtaining gypsum and CO_2 wet-scrubbing with organic amines obtaining carbamates. The latter leads to particular concern about, e.g. intensive energy requirements for desorption, corrosion of steel pipes and pumps, CO_2 absorption capacity and thermal decomposition of the amine.

In this work we demonstrate how ionic liquids (ILs) can be applied as selective, high-capacity absorbents of environmentally problematic flue gases like, e.g. SO_2, NO/NO_2 and CO_2. Reversible absorption has been obtained for several different ILs at different temperatures and flue gas compositions. The structures of ILs are well-ordered even in the liquid state with regular cavities which can host selected solute species depending on the IL ion composition. This makes the materials promising for selective, reversible absorption of gaseous pollutants in, e.g. power plant flue gases and other industrial off-gases (1,2). Furthermore, different porous, high surface area carriers like mesoporous silica and titania have been applied as supports for the ionic liquids to obtain Supported Ionic Liquid-Phase (SILP) absorber materials, Figure 1. These materials benefit from low mass transport resistance of the often highly viscous ILs by the distribution of the liquid as a thin film (or small droplets) on the surface of highly porous carrier materials which enable fast absorption/desorption rates of the particular gas exposed to the SILP absorber (3).

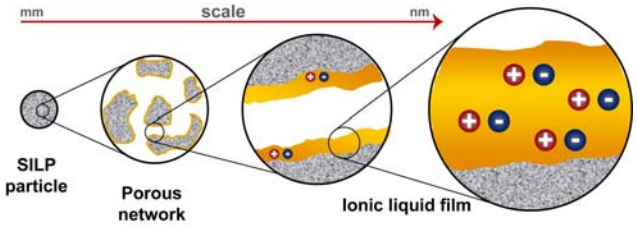

Figure 1. Principle of SILP materials.

Experimental

Materials

Synthesis of 1-butyl-3-methylimidazolium nitrate [BMIm]NO_3. 1-butyl-3-methyl-imidazolium nitrate was prepared using commercially available [BMIm]Cl (Fluka, >99%). The anion was exchanged by dissolving the [BMIm]Cl in water and adding a solution of silver nitrate in water to precipitate AgCl. Just below equivalent amounts of $AgNO_3$ was used to avoid silver pollution in the IL. After mixing, the solution was left overnight to ensure complete precipitation. The solution was then filtered (repeated 6 times) after gently heating to aid clotting of the precipitate. Finally, the water was removed under reduced pressure (10 mbar, 40°C) followed by heating under high vacuum resulting in clear viscous [BMIm]NO_3. The water content of the IL was measured by Karl Fisher titration to be 1.1%.

Synthesis of 1,1,3,3-tetramethylguanidinium chloride [TMGH]Cl. The 1,1,3,3-tetra-methylguanidinium chloride was prepared by direct neutralization of an ethanolic (99.9%, Aldrich) solution of TMG (99%, Aldrich) with hydrochloric acid (37%, Aldrich) (4). To an ice-bath cooled stirred solution of TMG (11.5 g, 0.10 mol) in ethanol (100 mL) concentrated hydrochloric acid (0.10 mol) was carefully added. Caution: neutralization of base with a strong acid is highly exothermic. After continuous stirring (25 °C, 24 h), the solvent was removed under reduced pressure with heating at 70°C followed by heating under high vacuum. The product was recrystallized in ethanol.

Synthesis of tetrahexylammonium prolinate [N6666][Pro]. 40 wt% aqueous solution of tetrahexylammonium hydroxide, [N6666]OH (13.92 g, 15 mmol, Sigma-Aldrich) and L-proline (1.89 g, 16 mmol, Sigma-Aldrich) was mixed and the solution stirred overnight at room temperature to ensure full deprotonation of the amino acid. Most of the water was removed under reduced pressure (10 mbar, 40 °C), and excess amino acid removed from the product by filtration after addition of cold acetonitrile (10 mL) and immersion into an ice bath for 1 h. Finally, the solvent was evaporated under reduced pressure to obtain the IL. The NMR and FT-IR spectra confirmed the identity of the ionic liquid. The purity of the IL was estimated by integration of visible impurities in the ^{1}H NMR spectrum. Yield > 99 %. Purity > 99 mol %.

Preparation of SILP absorbers. The SILP absorbers were prepared using fractioned (180-355 µm) silica, anatase and carbon support materials. The pore volume and specific area of the support materials were determined from nitrogen physisorption by BET

measurements on a Micromeritics ASAP 2020 pore analyser after out gassing the samples in vacuum at 200 °C prior to measurement (see Table I).

TABLE I. Characteristics of the SILP support materials.

Support material	Type	Surface Area (m^2/g)	Pore Volume (cm^3/g)
Carbon	Black Pearl 1400 (Cabot)	580	0.71
Anatase	ST 31119 (Saint-Gobain)	150	0.38
Silica	SS 611138 (Saint-Gobain)	251	0.93
Silica	Gel-90 (Fluka)	257	0.93

NO SILP absorbers were prepared by suspending support material in an excess of solvent (methanol for anatase and silica, dichloromethane for carbon) and then adding [BMIm]NO_3 corresponding to a pore volume filling degree of 25-30% to the mixture. After stirring the solvent was removed using a rotary evaporator. The evaporation was performed at slightly reduced pressure and ambient temperature in order to give the best possible distribution of IL on the surface of the support. In the case of silica (Saint-Gobain), two type of SILP absorbers were prepared; one with the fractioned silica as is and one with fractioned silica that had been calcined at 500 °C for 20 h and cooled to room temperature in a desiccator.

SO_2 SILP-absorbers were made in a similar way as the NO SILP absorbers by wet impregnation by an ethanolic solution of [TMGH]Cl on SiO_2 (Fluka). In the investigation only the absorption optimized SILP of 20 wt% was used.

Gas absorption methods

NO absorption: NO removal with SILP-absorbers was performed using a fixed-bed reactor system with about 3 g SILP absorber as outlined previously (5). A simulated flue gas containing 0.2 vol% NO (AGA) and 16 vol% O_2 in N_2 with and without ~2 vol% water was adjusted by Bronkhorst mass-flow controllers to a total flow of 50 ml/min and passed through the reactor interacting with all of the material. The reaction was followed by gas phase UV-Vis (Lambda 11 UV/Vis spectrophotometer) with a gas cuvette of path length 10 cm downstream of the reactor. The NO removal could be followed by integration of the characteristic lines from NO (227 nm) in the spectrum and comparison to the spectrum of the bypass flow. NO_2 and N_2O_5 were observable as a broad, slightly asymmetrical band at approximately 218 nm (NO_2) and a broad, symmetrical band centered at around 191 nm (N_2O_5). The amounts of these gases could not be quantified reliably by the same method.

SO_2 absorption: The measurements on the SO_2 SILP-absorbers were performed in a similar setup as used for the NO absorption studies (see above) using about 4 g of absorber and a dry or wet gas flow of 100 ml/min 3% SO_2 in N_2 (Air Liquide). The SO_2 concentration in the carrier stream was determined by UV-Vis (JACS V570 UV/Vis/NIR spectrophotometer).

CO_2 absorption: Absorption of CO_2 in different amino acid-based ILs was performed at 1 bar CO_2 at room temperature with 1.0-1.2 g ILs in bubble reactors by monitoring the mass increase on an analytic balance (Sartorius CPA324S, accuracy ±0.0001 g) at regular intervals.

Thermal methods

Enthalpy of fusion and heat capacity: Enthalpy of fusion (ΔH_{fus}) and heat capacity (C_p) were measured for SO_2 absorption with a DSC 111 SETARAM calorimeter. The temperature of the thermostat was measured by the resistance of a suitable Pt resistor, which was calibrated by the melting points of standards. All around the reference and the sample cylindrical cells were placed thermopiles of Tian-Calvet type, which consists of many thermocouples connected in series. At a given temperature, the voltage difference between the two thermopiles is proportional to the differential heat flux through the walls of the reference and the sample cells. By recording the thermogram the enthalpy of reaction or transformation can be measured. For an ideal instrument of perfect thermal symmetry, the differential heat flux is zero under constant temperature or dynamic changing temperature conditions. Asymmetries may arise from several effects: Static effects due to the ineluctable asymmetry in the cells and sensors and their location, which translate into a stationary flux recorded at any given temperature. The data processing must take the corrections of asymmetric heat flows into account.

C_p was measured by the step method which consists in programing the temperature and measuring differential heat fluxes between reference and sample cells. At each step the integration of the differential heat flux divided by the temperature step gives the value of C_p. First a blank experiment using empty sample containers was performed. Then, at the same temperature and time conditions a known mass of sample was added in the sample container and a similar run achieved. Calibration with a standard NBS-Al_2O_3 sample finished the measurement. An inaccuracy generally less than 5% is expected forenthalpy and C_p measurements.

Heat of gas absorption: The integral or partial enthalpies of dissolution of gases in liquids or solids (ΔH_{diss}) can be measured by direct reaction calorimetry. In an ambient temperature Tian-Calvet calorimeter, the sorbent was placed in a special glass cell containing a device for flowing a gas or a mixture of gases. The applied calorimeter was of classical design with thermopiles as described above, but including hundreds of thermocouples. The heat flux sensitive volume was 14 cm^3. The calorimeter with special characteristics of high sensibility (70 µW/µV) and very high stability (less than ± 20µW over several days) was used in isothermal mode up to 80 °C in a temperature controlled room at 19.5 ± 0.1 °C. The gas flow was controlled by Brooks mass-flow meters calibrated for SO_2 and Ar, respectively, at a sufficiently low flow not disturbing the heat flow of the calorimeter.

Results and Discussion

NO absorption

Recently, it has been found that NO can be absorbed and oxidized to nitric acid (HNO_3) in several ILs according to equation [1] (6,7).

$$4\ NO + 3\ O_2 + 2\ H_2O \rightarrow 4\ HNO_3 \qquad [1]$$

Water is needed in the reaction but it is also possible that water can inhibit the uptake of NO. It is most probable that the anion of the IL activates the otherwise unreactive NO

molecule by nucleophilic attack. Extensive hydrogen bonding is expected to take place when water is dissolved in the IL, possibly weakening the basicity and the nucleophilic strength of the anion. The identity of the cation of the IL does not seem to play any significant role for the rate nor the capacity (6). In analogous measurements with SILP materials containing other IL anions (results not shown) a different initial rate of uptake was found.

The initial absorption capacity (interpreted as the UV-silent time) of a SILP material consisting of [BMIm]NO_3 on anatase was determined at water:NO molar ratios of 1:1 and 10:1 in the gas corresponding to 2:1 and 20:1 in stoichiometric terms according to equation [1] (Figure 2). The initial uptake appeared to be largely independent of the water concentration, and no apparent inhibition was found when increasing the water content of the simulated flue gas. At steady state a small but significant decrease in NO_2 content in the effluent flue gas was observed. This is likely caused by a larger fraction of the NO_2 molecules reacting with water according to equation 2.

$$2NO_2 + H_2O \rightarrow HNO_3 + HNO_2 \qquad [2]$$

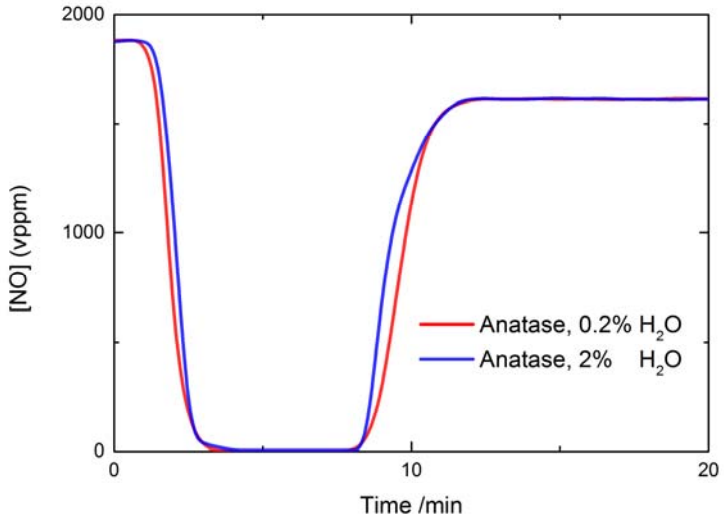

Figure 2. Concentration of NO measured downstream of the absorber for an anatase SILP with a water:NO molar ratio of 1:1 (0.2 % water) and 10:1 (2 % water).

The absorption reaction was also investigated with lower than stoichiometric amounts of water and examples of resulting spectra after breakthrough are shown in Figure 3 for a carbon and a (uncalcined) silica based SILP, respectively. The broad absorption band seen in Figure 3 is interpreted as N_2O_5. It is usually observed in the absorption spectra when the water content of the flue gas is low. The amount of N_2O_5 increased significantly when applying more hydrophobic supports (e.g. carbon) for the SILP absorber. The formation of N_2O_5 under dry conditions is suggested to be facilitated by ionization of N_2O_4 to NO_2^+ and NO_2^- in the IL (6). The formed NO_2^+ can undergo further reaction with NO_3^- from the IL to form N_2O_5 observed in the gas phase downstream of the absorber. When water is present both the N_2O_4 and the N_2O_5 dissolved in the IL reacts with water, leading to formation of HNO_3 which accumulates in the IL due to the formation of strong symmetric hydrogen bonds with the nitrate anion.

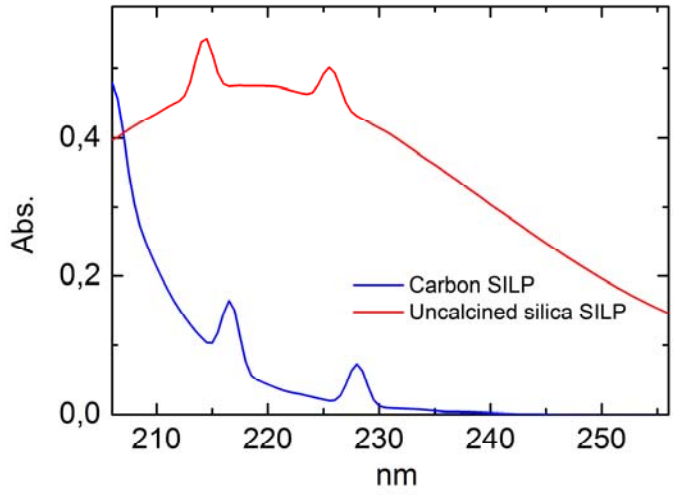

Figure 3. Post-breakthrough spectral data at sub-stoichiometric amounts of water, for two different SILP formulations.

SO_2 absorption

Figure 4 shows the results of the absorption measurements of 0.15 % of SO_2 in dry N_2 and with 2 % water vapour at 30 °C for a SiO_2 based SILP absorber with 20 wt% [TMGH]Cl. The figure shows the amount of SO_2 (mmol) detected in the gas stream after the absorber as a function of time. In the experiment the gas stream was initially bypassing the absorber and directed to the detector and after 10 min the gas flow was led to the reactor with the absorber material. From Figure 4 it is seen that the concentration of SO_2 in the gas stream dramatically drops after the gas flow was shifted from the bypass to the reactor with the absorbent. It is also seen that when the saturation of the investigated material with SO_2 is completed, the concentration of SO_2 in the outlet gas began to increase. After ca. 80 min of the reaction the concentration of SO_2 in the outlet gas was identical to the concentration of SO_2 in the inlet gas.

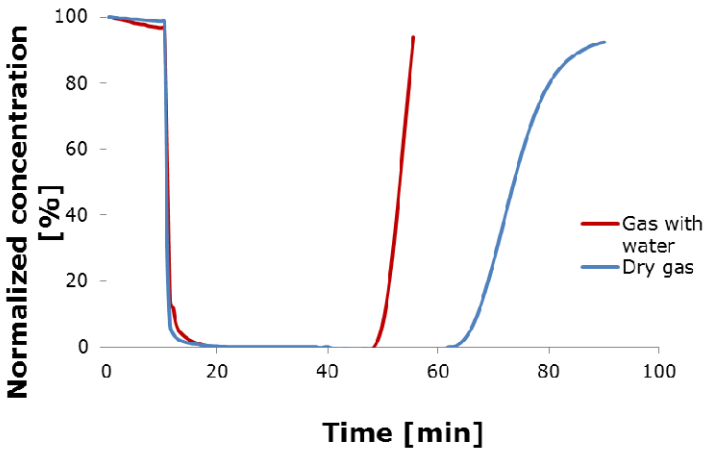

Figure 4. SO_2-absorption by 20 wt% [TMGH]Cl-SiO_2 SILP absorber in dry 0.15 % SO_2/N_2 and this gas saturated with water (3 %) until breakthrough.

The total absorption capacity for SO_2 (1500 ppm in N_2) for the 20 wt% [TMGH]Cl-SiO_2 SILP absorber at the given conditions is determined by integration of the area of absorption within the curve from 10 to ca. 80 min to be 0.05 mole fraction SO_2 in the IL for the dry gas and reduced by ca. 35% in the wet gas. The absorber material was tested by absorption and desorption of SO_2 up to 10 times in the dry gas without any significant changes in the absorption capacity as shown in our previous work (5).

Based on a X-ray investigation of crystals obtained of the SO_2 adduct [TMGH]Cl·SO_2, we previously suggested strong interaction between Lewis basic chloride ions and the Lewis acidic SO_2 molecules to account for the high absorption affinity of the salt (4). With water present in the gas the capacity is significantly reduced probably due to competition between water molecules and SO_2 regarding coordination to Cl^-. This scenario will be further elucidated by ongoing Raman spectroscopic investigations. However, thermal investigations allowed providing insight about the energy of these interactions in dry and wet gases.

Thermal investigations of SO_2 and H_2O absorption

The DSC investigations were performed on samples of 60-80 mg of [TMGH]Cl loaded in a dry box into aluminium capsules and sealed airtight by pressing an aluminium lid into the capsule using a Ni-joint. The thermogram (DTA) was run in the range 26-225 °C at a rate of 1 °C/min. The thermogram exhibited one endothermic peak corresponding to the fusion of [TMGH]Cl at 205 °C in good accordance with the previously reported value of 208-209 °C (4).

The heat of fusion (ΔH_{fus}) of [TMGH]Cl was found to be 22.5 kJ/mol. There is no value in the literature to compare with as far as we know. The measured heat capacities (C_p) varied in the range 200-300 J/mol·K for the solid state, expressed by the polynomium 191 + 0.645·T in the temperature range 26-176 °C, and is equal to 420 J/mol·K within the experimental error for the liquid state in the short interval 206-225 °C.

In Figure 5 the thermograms obtained on [TMGH]Cl at 25 °C in the calorimeter under a flow of dry SO_2 gas and humid gas (2.3% H_2O in SO_2) at 1 bar total pressure are shown. The absorption of dry SO_2 gas lead to a strong exothermic effect, which by integration after calibration by heat pulses from an electrical resistance in contact with the experimental cell, gives a value of 90.35 kJ/mol for the heat of absorption of [TMGH]Cl. By weighing of the solid sample after the experiment the mole ratio of SO_2:[TMGH]Cl in the solid in the cell was found to be 1.15. These values were found to be 74.66 kJ/mol and 1.19 at 50 °C and 9.62 kJ/mol and 0.40 at 84 °C, respectively, indicating an increasingly weaker bonding of SO_2 by increasing temperature.

The absorption of humid SO_2 gas in [TMGH]Cl at 25 °C leads to an exothermic peak as well, but with a heat of absorption of 145.73 kJ/mol. The kinetics of the absorption process was obviously different for the two experiments being very slow in the humid gas only obtaining equilibrium after several days, while the dry gas absorption process was much faster taking only a few hours to reach equilibrium, as realized by blow up of the tail end of the thermograms (not shown). A marked difference was that the final product after humid gas exposure was a liquid, while it was a solid up to around 85 °C in dry gas

where it starts to melt incongruently under 1 bar dry SO_2. This solid is presumably the adduct compound TMGH]Cl·SO_2, which structure has been described recently (4).

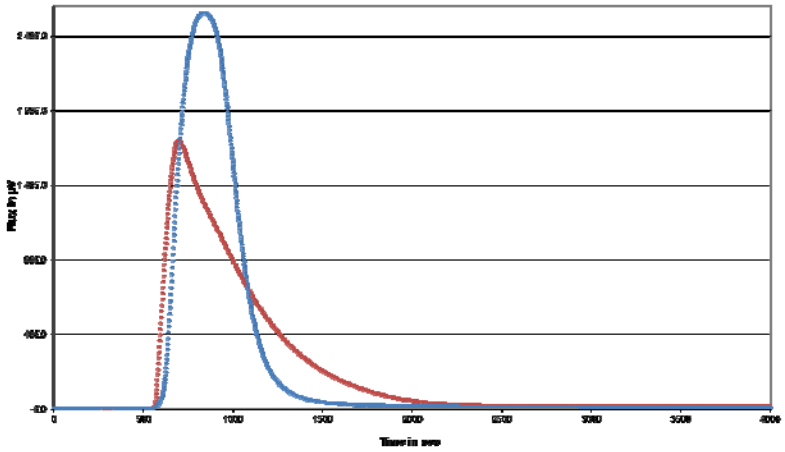

Figure 5. Thermograms (selected time period) of 1 mmol [TMGH]Cl in dry SO_2 (blue) and in humid SO_2 with 2.3 % H_2O vapor (red) at 25 °C with gas flow of 5.0 ml/min.

The absorption process in the humid gas comprised two components: A fast exothermic coordination of SO_2 to the solid TMGH]Cl followed by a slower uptake and less exothermic absorption of H_2O eventually leading to fusion of the mixture. The quantification of the equilibrium mole ratio SO_2:[TMGH]Cl in the humid gas at equilibrium is in progress. Desorption by a flow of dry Ar through the cell at 25-50 °C is a slow process leading to almost the same enthalpy as for the absorption, but slightly lower indicating that it was difficult to completely remove the absorbed components. However, successive absorption of SO_2 appeared completely reversible in this temperature range. From previous measurements on SILP absorbers (3) it is obvious that fast and reversible desorption can be performed by raising the temperature to 120 °C in a flow of, e.g. N_2 or air.

In a separate experiment at 25 °C with a flow of Ar and 2.3 % H_2O vapour, again a rather fast exothermic absorption of water by [TMGH]Cl was observed followed by a very slow further absorption of water reaching equilibrium only after several days. Again the solid was transformed to a liquid. Here the weight increase corresponded to a molar ratio H_2O:[TMGH]Cl of 4.42 and a heat of absorption of 289 kJ/mol [TMGH]Cl or 65.3 kJ/mol H_2O. This latter value is significantly higher than the heat of vaporization of water of 43.9 kJ/mol also at 25 °C. This indicates a much stronger interaction of the H_2O molecules with the ions in the formed IL, than in pure water at the same conditions. Further progress on the thermal measurements is expected in the near future.

<u>CO_2 absorption</u>

Previous results from our group for CO_2 absorption by amino acid-based ILs show a super-stoichiometric uptake of CO_2 (8). The effect of water on the ILs ability to take up

water is explored here. Water content seems to play an important role for CO_2 absorption by amino acid-based ILs. Not only does it lower the ILs viscosity, but it also seems to have a large positive effect on the CO_2 absorption stoichiometry and -rate. This can be seen for the IL [N6666][Pro] in Table II and Figure 6.

TABLE II. Effect of water on CO_2 absorption capacity in neat [N6666][Pro] IL at room temperature.

Entry	Ionic liquid	Water content (qualitative assessment)	CO_2 absorption stoichiometry (mol CO_2/mol IL)
1	[N6666][Pro]	Wet[a]	0.71
2	[N6666][Pro]	Dried[b]	0.38
3	[N6666][Pro]	Very dry[c]	0.93

[a] Dried at 15 mbar for 1 h. Probably 5-10 % water. [b]Dried at 1 mbar for 24 h. Probably 1-2 % water. [c] Dried at 1 mbar for 24 h followed by three freeze-pump-thaw cycles. Water content measured to be < 0.01 % by Karl-Fischer.

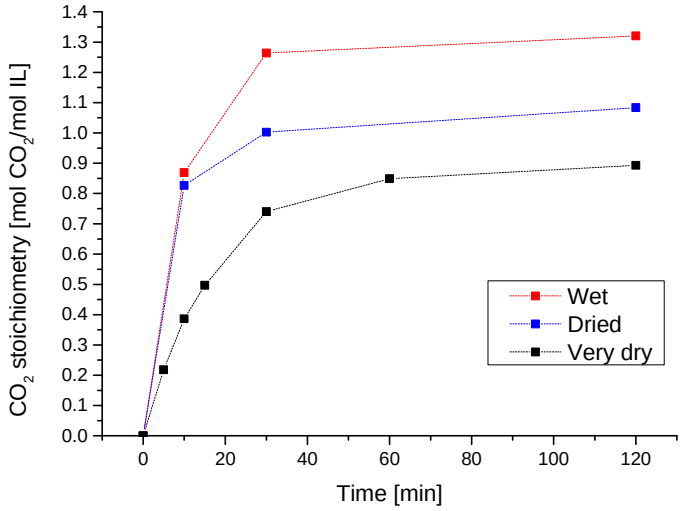

Figure 6. CO_2 absorption capacity in [N6666][Pro] at room temperature as a function of time with varying degrees of IL dryness (see Table II).

In the experiment, all mass at time zero was assumed to be IL and the absorption stoichiometries have been calculated accordingly, despite that a significant percentage of the wet sample was water. Surprisingly, a higher water content was not only associated with a higher CO_2 uptake stoichiometry, but seems to be a prerequisite for the previously reported super stoichiometric CO_2 uptake (8). The solubility of CO_2 in pure water at 25 °C and 1 atm is only $6 \cdot 10^{-4}$ mol per mol of H_2O (9). Hence, this low value cannot account for the added CO_2 absorption, but the water content in the IL is most likely responsible for the super stoichiometric CO_2 uptake.

CO_2 absorption in the samples was measured by mass increase, but it can be hard to correct for a possible loss of weight from evaporation of water. Therefore, an experiment was devised in which the CO_2 absorption of the very dry sample was compared to that of a sample absorbing from a gas stream that had been pre-saturated with water by passing the gas through a wash bottle with water at room temperature. Absorption from both wet CO_2 and wet Ar gas was followed, and it is assumed that the water content in the gas streams were identical. This can be seen from Figure 7. The sample in the wet Ar stream

did not - strictly speaking - take up CO_2, but as “stoichiometry” scales linearly with weight it allowed directly comparison of the samples.

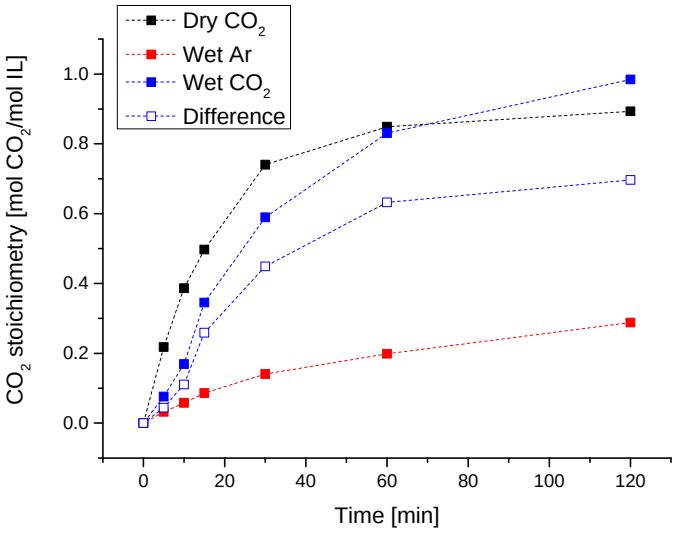

Figure 7. Uptake of CO_2 by dry [N6666][Pro] at room temperature during absorption in dry CO_2 (black), in wet Ar (red) and in wet CO_2 (blue, full), as well as in wet CO_2 corrected for mass increase in wet Ar (blue, open).

The mass of the sample in wet CO_2 did not increase more rapidly than the sample in dry CO_2. This is in agreement with experiments performed with 1,1,3,3-tetramethyl-guanidinium imidazolate [TMGH][Im], where presence of water slowed down the CO_2 absorption (10). A first impulse would be that the IL at first is “busy” taking up water, and it only gains absorption momentum later, which is in agreement with a minimum amount of water being needed for rapid uptake of CO_2.

Figure 8. Absorption stages in dry [N6666][Pro]. The IL is initially transparent (left) but a turbid phase appeared during absorption (right).

A possible explanation for the difference in absorption stoichiometry and rate in the presence of pre-absorbed water (Table II and Figure 7), is possibly that water facilitate a different mechanism for uptake of CO_2 that is not available in a dry gas stream. This is supported by the qualitative assessment of the ILs upon CO_2 absorption. During absorption, a turbid phase appeared in the dried and very dry samples after absorbing 1.00 and 0.38 equivalents, respectively (see Figure 8). This turbid phase did not appear

during absorption in the wet sample. This suggests that pre-absorbed water has a highly positive influence on CO_2 absorption in amino acid-based ILs. For some reason, concerted absorption of water and CO_2 did not see this positive effect – possible because water was not absorbed sufficiently fast.

Conclusions

The presented results demonstrate that NO/NO_2, SO_2 and CO_2 can be absorbed by ILs through different mechanisms of absorption. Furthermore, impregnation of porous solids to make Supported Ionic Liquid-Phase (SILP) absorbers leads to solid materials with good absorption/desorption dynamics. However, water plays a significant role for the absorption processes and the absorption capacities regarding the different gases and the investigated ILs.

Unlike separation of other acidic gases (e.g. SO_2 and CO_2) using ILs, NO absorption and oxidation in IL-based materials is less dependent on the nature of the anion. It is also less affected by the presence of large amounts of water in the gas flow. Water is necessary to provide the final product - nitric acid - but the reaction can also proceed under relatively dry conditions. In this case, the products are more dominated by the anhydrous oxidation products N_2O_4 and N_2O_5. The observation that a large excess of water is not detrimental to the removal of NO is a big advantage for deNOx applications, since most flue gases contain large quantities of water. Furthermore, the hydrated conditions might hinder or slow down possible accumulation and poisoning of the NO absorbers by other acidic gases. Regarding absorption of SO_2 and CO_2 initially the presence of water is similarly not a drawback. It may even enhance the kinetics of absorption until saturation, but further uptake of water may lead to increasingly substitution of the absorbed molecules, thus decreasing the overall capacity for the flue-gas absorption.

The absorption/desorption process may be performed by SILP materials shaped in honey comb structures as the traditional SCR deNO_X catalyst used in power plants today, leading to optimized gas diffusion and low pressure drop of the passing flue gas. Installed as a traditional rotating heat exchanger it will facilitate desorption by elevation of the temperature in a smaller side channel and make it possible to desorb the gases in concentrated form.

Acknowledgments

Energinet.dk, DONG Energy A/S, Vattenfall A/S, LAB S.A. Lyon, France and the Danish Maritime Fund are greatly acknowledged for financial support.

References

1. J. Huang, A. Riisager, P. Wasserscheid and R. Fehrmann, *Chem. Commun.*, 4027 (2006).
2. W. Wu, B. Han, H. Gao, Z. Liu, T. Jiang and J. Huang, *Angew. Chem. Int. Ed.*, **43**,

2415 (2004).
3. S. Shunmugavel, S. Kegnæs, J. Due-Hansen, T. A. Gretasdottir, A. Riisager and R. Fehrmann, *ECS Trans.*, **3**, 49 (2007).
4. R.W. Berg, P. Harris, A. Riisager and R. Fehrmann, *J. Phys. Chem.* A, **117**, 11364 (2013).
5. P. Thomassen, A.J. Kunov-Kruse, S. Mossin, H. Kolding, S. Kegnæs, A. Riisager and R. Fehrmann, *ECS Trans.*, **50**, 433 (2012).
6. S. Mossin, A.J. Kunov-Kruse, P. Thomassen, A. Riisager and R. Fehrmann, submitted.
7. A. Riisager, A. J. Kunov-Kruse, S. Mossin and R. Fehrmann, Patent Application *EP11191127.7* (2011).
8. H. Kolding, A. Riisager and R. Fehrmann, *Sci. China Chem.*, **55**, 1648 (2012).
9. J.J. Carroll, J.D. Slupsky and A.E. Mather, *J. Phys. Chem. Ref. Data*, **20**, 1201 (1991).
10. X. Lei, Y. Xu, L. Zhu and X. Wang, *RSC Adv.*, **4**, 7052 (2014).